

Effect of nitro content on thermal stability and decomposition kinetics of nitro-HTPB

Hadi Abusaidi¹ · Hamid Reza Ghaieni¹ · Seied Mahdi Pourmortazavi² · Seied Hadi Motamed-Shariati¹

Received: 24 April 2015 / Accepted: 22 November 2015 / Published online: 11 December 2015
© Akadémiai Kiadó, Budapest, Hungary 2015

Abstract This paper has been utilizing the simultaneous thermogravimetric analysis and differential scanning calorimetry (TG–DSC) to investigate the thermal decomposition of nitro-HTPB as an energetic binder. Data on thermal stability along with the decomposition kinetics of energetic materials are required to better comprehend their decomposition mechanism and the hazards involved in their handling, storage and processing. The thermal behaviors of different nitro-HTPB samples with various nitro group contents were determined. Decomposition kinetic was investigated by evaluating the influence of DSC heating rate (10, 20, 30 and 40 °C min⁻¹) on the behavior of a nitro-HTPB sample. The results as expected showed that the decomposition temperature of the nitro-HTPB decreases with the increase in the DSC heating rate, while thermal decomposition of the sample followed a first-order law. The kinetic and thermodynamic parameters of the nitro-HTPB decomposition under ambient pressure were obtained from the resulted DSC data via non-isothermal methods proposed by ASTM E698 and Flynn–Wall–Ozawa. Also, the critical temperature of the nitro-HTPB was estimated at about 181 °C.

Keywords Nitro-HTPB · Thermal stability · TG–DSC · ASTM · FWO · Non-isothermal kinetic

Introduction

The principles behind the usage of the energetic binders in propellant and explosive formulations are defined by the energetic performance with the emphasis on their retaining properties [1]. The suitability of energetic polymers employment as the binder to improve the safety, the correlated problems with their preparation, the performance and the properties has been discussed in details, previously [1–3]. The efficiency and performance of the plastic-bonded explosives (PBXs) and propellants is dependent on the surface area, physical feature and the mechanical properties of the resulted materials, and so frequently a binder is utilized in their formulations to improve the properties [1]. The modern composite propellants and PBXs utilize the hydroxyl-terminated polybutadiene (HTPB) as a binder due to its precise properties, i.e., brilliant flow properties and substantial capacity compared with the similar binders [3]. HTPB has been utilized in the energetic formulations since 1989 as a curable and crosslinkable prepolymer due to the desirable mechanical properties of polyurethane presented in the polymer structure [4]. Different commercially available explosive products are trained with the HTPB in propellants [2–4]. HTPB possesses the excellent physical properties for employment as a binder in explosive charges and reduction in their vulnerability; however, it has some uninteresting problems. Due to the inert nature of this binder, the explosive dilutes by its usage and hence reduces the overall energy content and also the performance. HTPB could load only about 92 % solid materials in the propellant formulation, while 8 % is remained [5]. The limitations of HTPB make the development of energetic binders inevitable, though by introducing the energetic functionalities [4–6]. In order to retain or improve the total energy and performance of the explosive formulations, the recent

✉ Seied Mahdi Pourmortazavi
poumortazavi@yahoo.com

¹ Department of Chemistry and Chemical Engineering, Malek Ashtar University of Technology, Tehran, Iran

² Faculty of Material and Manufacturing Technologies, Malek Ashtar University of Technology, Tehran, P.O. Box 16765-3454, Iran

trend is the employment of energetic binders, i.e., nitrated HTPB, GAP, poly(NIMMO) and poly(GLYN) in PBXs and composite propellant formulations. Among the mentioned energetic binders, a considerable attention has been paid on the nitration of HTPB to achieve higher energy contents [7–19]. Thermal analysis investigation on high energetic materials is suitable to appreciate the kinetic and the mechanism of their thermal decomposition and evaluate the potential hazards of their exothermic decomposition during processing, handling and storage [20–24]. Furthermore, thermokinetic studies afford interested information on thermal stability and shelf life of the energetic materials to store at definite conditions [25, 26]. During this investigation, thermal stability and decomposition kinetics of the nitro-HTPB samples with different Nitro contents were studied by simultaneous thermogravimetric analysis and differential scanning calorimetry (TG–DSC).

Experimental

Nitro-HTPB samples with different contents of the nitro function (i.e., 9.4, 12.5, 14.2, 16.1 and 17.3) were synthesized as proposed previously by Ref. [27]. The synthesized samples were characterized by NMR. Thermochemical behaviors of the nitro-HTPB samples were characterized by a METTLER TOLEDO differential scanning calorimeter, model TG/DSC 1. All binder samples were analyzed by DSC/TG using an aluminum crucible under nitrogen atmosphere with the purge flow rate of 50 mL min^{-1} and heating rate of $10 \text{ }^\circ\text{C min}^{-1}$ at the temperature range of 50–600 $^\circ\text{C}$. The sample mass used in each test was 5.0 mg. The DSC experiments were carried out on nitro-HTPB sample with the highest nitro content (17.3 %) at the temperature range of 50–600 $^\circ\text{C}$ and different heating rates (i.e., 10, 20, 30 and $40 \text{ }^\circ\text{C min}^{-1}$).

Results and discussion

Thermal decomposition of nitro-HTPB

Figure 1 shows the resulted TG/DSC curves of the 17.3 % nitro-HTPB heated at the rate of $10 \text{ }^\circ\text{C min}^{-1}$. This nitro-HTPB sample undergoes an exothermic decomposition with the maximum peak temperature $225.8 \text{ }^\circ\text{C}$, which is accompanied with a heat release of 1024 J g^{-1} . Mass loss of the sample during this exothermic event was about 75 %. It has been reported [28] that thermal decomposition of the nitroalkenes at this temperature is due to the loss of NO_2 groups in the form of HNO. The further mass loss of this sample at higher temperature is responsible for the

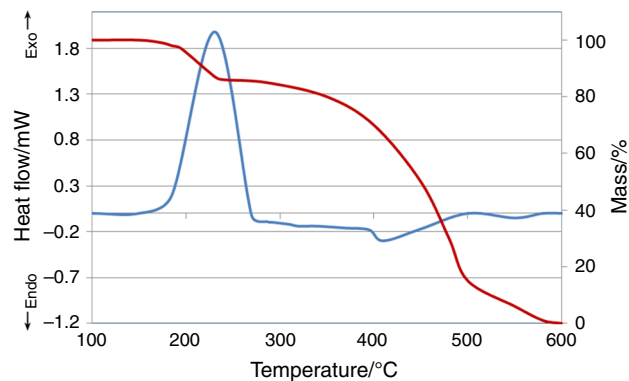


Fig. 1 DSC/TG curves of nitro-HTPB with nitro content of 17.3 % (sample 1); sample weights 5.0 mg; heating rate $10 \text{ }^\circ\text{C min}^{-1}$; nitrogen atmosphere

decomposition of the hydrocarbon backbone of polymer similar to the pure HTPB sample.

Effect of DSC heating rate on decomposition of nitro-HTPB

Figure 2 shows the resulted DSC curves of the nitro-HTPB with 17.3 % nitro content (sample 1) at several heating rates (i.e., 10, 20, 30 and $40 \text{ }^\circ\text{C min}^{-1}$). As seen, the decomposition temperature of the nitro-HTPB was shifted to the higher temperatures by increasing the DSC heating rate. These shifts in the values of onset temperature and maximum peak temperature are shown in Fig. 3. On the other hand, the results of our study show that as the DSC heating rate was increased, the heat of decomposition resulted from the peak area was increased. These increments in the heat of decomposition are presented in Fig. 4.

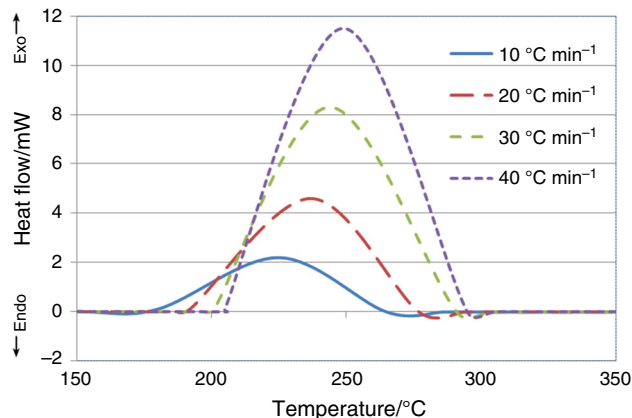


Fig. 2 Effect of heating rate on the DSC results of nitro-HTPB with 17.3 % nitro content (sample 1); sample mass 5.0 mg; nitrogen atmosphere

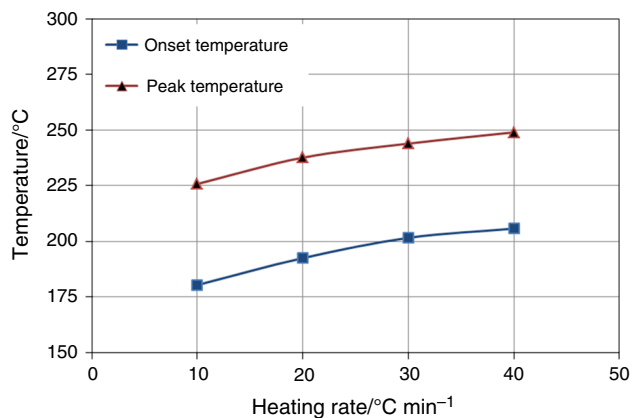


Fig. 3 Variation of onset temperature and peak temperature of nitro-HTPB with 17.3 % nitro content (sample 1) by changing heating rate

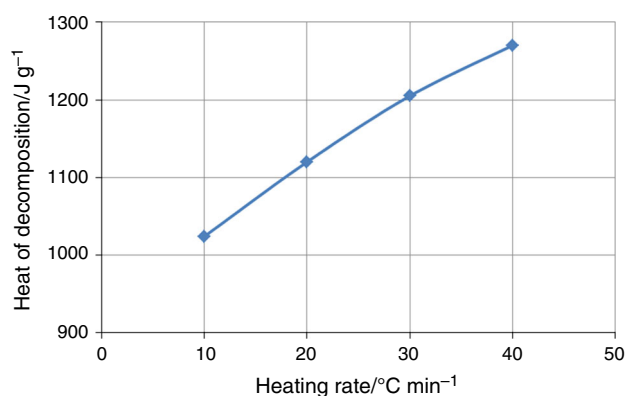


Fig. 4 Effect of various heating rate on heat of decomposition for nitro-HTPB with 17.3 % nitro content (sample 1)

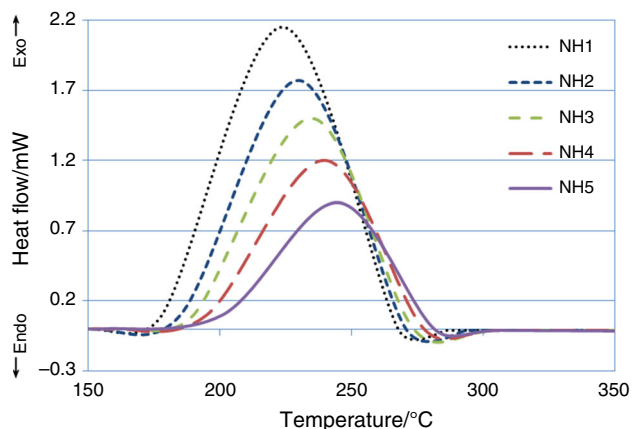


Fig. 5 Effect of nitro content of nitro-HTPB on DSC behavior (the nitro content of the samples was NH1: 17.3, NH2: 16.1, NH3: 14.2, NH4: 12.5 and NH5: 9.4 %)

Effect of nitro content on thermal decomposition of samples

Figure 5 shows DSC curves of the nitro-HTPB samples with various nitro contents at the heating rate of $10\text{ }^{\circ}\text{C min}^{-1}$. As seen, the sample with 9.4 % nitro content has the highest thermal stability, while the sample containing 17.3 % nitro possesses the lowest thermal stability. It was found that the thermal stability of nitro-HTPB decreases with increasing its nitro content. The variations in the onset temperature and maximum peak temperature of different samples are shown in Fig. 6. Also, the results of this study showed that as the nitro content of nitro-HTPB samples was increased, the heat of decomposition resulted from the DSC peak area was increased. These increments in the heat of decomposition are presented in Fig. 7.

Kinetic of nitro-HTPB thermal decomposition

The thermokinetic parameters corresponding to the thermal decomposition of the nitro-HTPB sample with 17.3 % nitro content were determined by DSC data and using the ASTM method E698 [29]. The DSC curves of the nitro-HTPB sample obtained at different heating rates are shown in Fig. 2. The resulted data from this figure were used to plot the $\ln(\beta T_p^{-2})$ versus T_p^{-1} , and the obtained plot is presented in Fig. 8. It could be found that plotting of $\ln(\beta T_p^{-2})$ against T_p^{-1} was a straight line for the studied nitro-HTPB sample, which indicates that the mechanism of thermal decomposition reaction is the first order [30–32].

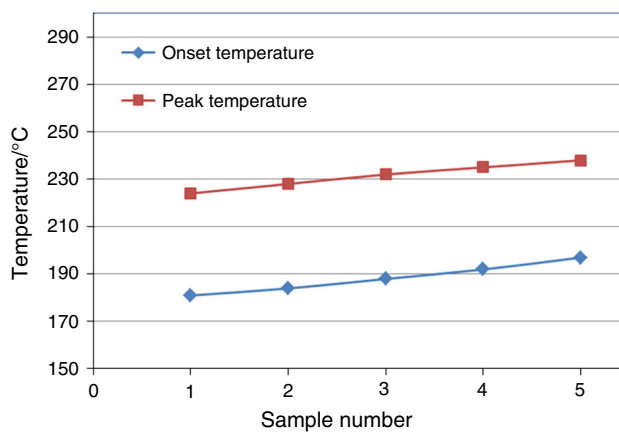


Fig. 6 Effect of nitro content of nitro-HTPB on the onset temperature and peak temperature of decomposition process (the nitro content of the samples was sample 1: 17.3, sample 2: 16.1, sample 3: 14.2, sample 4: 12.5 and sample 5: 9.4 %)

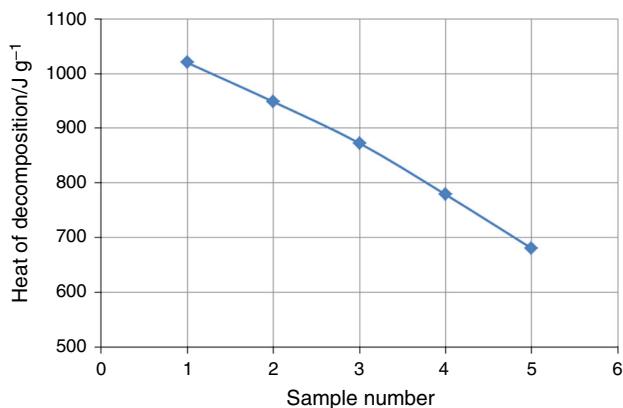


Fig. 7 Effect of nitro content of nitro-HTPB samples on the heat of decomposition

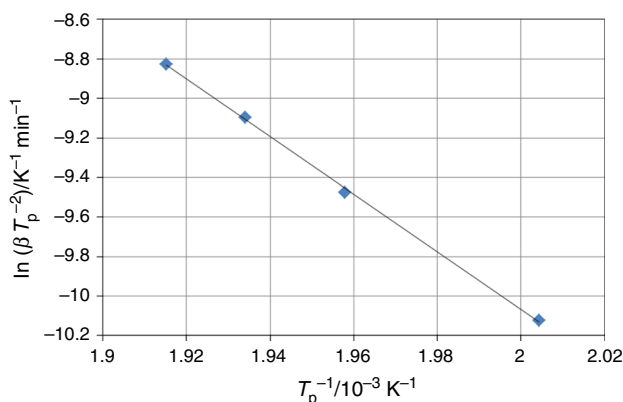


Fig. 8 Plot of $\ln(\beta T_p^{-2})$ versus T_p^{-1} for the 17.3 % nitro-HTPB sample

As proposed by the ASTM method, the slope of this line is equal to $-E_a R^{-1}$. Therefore, the value of the activation energy (E_a) was obtained from the slope of this graph, while the pre-exponential factor, $\log(A/s^{-1})$, as another Arrhenius parameter was computed from the following expression given in ASTM E698:

$$A = \beta(E_a R^{-1} T_m^{-2}) \exp(E_a R^{-1} T_m^{-1}) \quad (1)$$

The calculated values of activation energy and frequency factor for the 17.3 % nitro-HTPB are listed in Table 1. Also, a second method was utilized to achieve the activation energy and frequency factor values for comparison. Based on the kinetics equations used for

heterogeneous chemical reactions, Flynn, Wall and Ozawa (FWO) [33–38] have been proposed a method to determine the kinetic parameters using TG/DSC curves, which so-called isoconversional method. The FWO method is based on the isoconversional principle which describes the rate of reaction at a constant extent of the conversion is only a function of the temperature. The Flynn, Wall and Ozawa method could be described by the following equation:

$$\log \beta = \log \frac{A E_a}{R g(\alpha)} - 2.315 - 0.4567 \frac{E_a}{R T_m} \quad (2)$$

where $G(\alpha)$ is the conversion functional relationship and the other terms possess their usual meaning. The degree of conversion could be defined as $\alpha = (m_0 - m)(m_0 - m_f)^{-1}$, while m_0 , m and m_f are corresponding to the initial, actual and the final mass of the sample. FWO as the isoconversional method permits to evaluate the dependence of the activation energy on the degree of conversion without the precise knowledge about $G(\alpha)$ [39]. At the maximum peak temperature, the degree of conversion (α) at different heating rates possesses a constant value [31]. Thus, de Doyle's approximation [33] could be applied on Eq. (2) to simplify it, and hence, Flynn, Wall and Ozawa rewrote this equation as:

$$\log \beta = \text{Const.} - 0.4567 \frac{E_a}{R T_m} \quad (3)$$

The value of activation energy corresponding to the decomposition of 17.3 % nitro-HTPB was predicted using FWO method. As shown in Fig. 9, plotting of the logarithm of heating rate values against reciprocal of the maximum peak temperature for the 17.3 % nitro-HTPB sample yields a straight line with $r^2 = 0.9993$. This result confirms that the thermal decomposition mechanism of the sample (17.3 % nitro-HTPB) undergoes no variation at the studied rates [33]. Meantime, the value of the frequency factor (A) for the sample might be computed via Eq. (1). The resulted kinetic data are presented in Table 1. The resulted data by both methods were compared. It was found that the calculated values by ASTM are faintly lower than those by FWO method. Furthermore, thermodynamic parameters of the activation for the decomposition reaction of 17.3 % nitro-HTPB are calculable from the resulted kinetic parameters (E_a and A), using the following equations [35, 36, 40]:

Table 1 Kinetic and thermodynamic parameters of the 17.3 % nitro-HTPB sample obtained by ASTM and FWO methods

Methods	Activation energy/ kJ mol ⁻¹	Frequency factor log A/min ⁻¹	Linear regression/ <i>r</i>	ΔG^\ddagger /kJ mol ⁻¹	ΔH^\ddagger / kJ mol ⁻¹	ΔS^\ddagger / J mol ⁻¹	$t_{1/2}$ / year	T_b /°C
ASTM	121.4	29.41	0.9992	106.0	117.0	21	9.2	181.4
FWO	123.5	29.91	0.9993	108.0	119.0	26	11.2	181.1

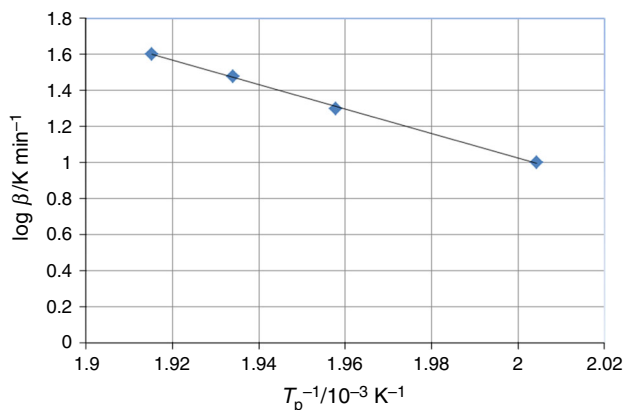


Fig. 9 Plot of $\log \beta$ versus T_p^{-1} for the 17.3 % nitro-HTPB sample

$$A \exp \frac{-E_a}{RT} = \nu \exp \frac{-\Delta G^\ddagger}{RT} \quad (4)$$

$$\Delta H^\ddagger = E_a - RT \quad (5)$$

$$\Delta G^\ddagger = \Delta H^\ddagger - T\Delta S^\ddagger \quad (6)$$

where ΔG^\ddagger , ΔH^\ddagger and ΔS^\ddagger represent the free energy, enthalpy and entropy of the activation, respectively; $\nu = k_B T h^{-1}$ (while k_B and h are, respectively, the Boltzmann and Planck constants). Calculated values of thermodynamic parameters for the nitro-HTPB sample are also presented in Table 1.

Half-life prediction

Based on the resulted kinetic parameters (E_a and A) and assuming first-order reaction, the value of the reaction rate

constant (k) for decomposition of the nitro-HTPB can be computed by the following equation [41, 42]:

$$\text{Log } k = \log A - E_a 2.3R^{-1}T^{-1} \quad (7)$$

Meantime, the half-life of the 17.3 % nitro-HTPB might be predicted by the upcoming equation:

$$t_{1/2} = 0.693k^{-1} \quad (8)$$

where k represents the reaction rate constant and this term is calculable from Eq. (7). At the temperature of 50 °C and utilizing the values of activation energy (E_a) and frequency factor (A) resulted in the above, Eq. (8) was solved. The resulted values of half-life for the 17.3 % nitro-HTPB sample are given in Table 1. As seen, this value for the 17.3 % nitro-HTPB sample at 50 °C is about 10 years.

Critical explosion temperature

In order to safe employment of the energetic materials in the explosives, propellants and pyrotechnic formulations, critical explosion temperature (T_b) is an essential parameter. This factor is defined as the lowest temperature at which a definite compound undergoes thermal run away [43, 44]. T_b is calculable based on the theory of inflammation and also some thermokinetic parameters, i.e., activation energy, heat of reaction and pre-exponential factor. Prediction of the critical temperature (T_b) for the 17.3 % nitro-HTPB is carried out by the corresponding equations as follows [44–46].

$$T_e = T_{e0} + b\beta_i + c\beta_i^2, \quad i = 1 - 4 \quad (9)$$

Table 2 Comparison of onset temperature and peak temperature of nitro-HTPB with nitrated HTPB (NHTPB) and nitrocellulose, heating rate 10 °C min⁻¹

Compound	Functional group	Maximum content/%	Onset temperature/°C	Peak temperature/°C
Nitro-HTPB	NO ₂	17.3	180	225
NHTPB [47]	ONO ₂	10	167	199
Nitrocellulose [35]	ONO ₂	13.9	188	210

Table 3 Comparison of kinetic and thermodynamic parameters of nitro-HTPB with NHTPB and nitrocellulose

Compound	Methods	Activation energy/ kJ mol ⁻¹	Frequency factor log A/min ⁻¹	Linear regression/r	$\Delta G^\ddagger /$ kJ mol ⁻¹	$\Delta H^\ddagger /$ kJ mol ⁻¹	$\Delta S^\ddagger /$ J mol ⁻¹	$t_{1/2} /$ year	$T_b /$ °C
Nitro-HTPB	ASTM	121.4	29.41	0.9992	106.0	117.0	21	9.2	181.4
	FWO	123.5	29.91	0.9993	108.0	119.0	26	11.2	181.1
NHTPB [47]	ASTM	173.98	19.13	0.9914	121.14	170.25	109.64	21.31	153.94
	FWO	173.46	19.07	0.9979	121.12	169.74	108.52	20.10	153.96
Nitrocellulose [35]	ASTM	156.8	16.89	0.9925	121.41	152.88	66	6.7	196.75
	Ozawa	154.0	16.58	0.9917	121.38	150.01	60	4.7	196.95

$$T_b = \frac{E_a - \sqrt{E_a^2 - 4E_aRT_{e0}}}{2R} \quad (10)$$

where b and c are the coefficients, while β_i is the utilized heating rate, R is the value of universal gas constant, and E_a represents the activation energy. T_{e0} represents the onset temperature, or T_e when $\beta_i \rightarrow 0$ and is given by Eq. (9). The computed value of T_{e0} is 167.25 °C for the 17.3 % nitro-HTPB. Then, the value of the critical temperature (T_b) was predicted from Eq. (10). The resulted values were 181.4 and 181.1 °C for the 17.3 % nitro-HTPB, respectively, by the employment of corresponded ASTM and FWO data.

Comparison of thermal data with previous studies

The thermal analysis results of 17.3 % nitro-HTPB were compared with nitrated HTPB (NHTPB) and nitrocellulose containing maximum ONO_2 content [35, 47]. These comparative results are presented in Tables 2 and 3. The values of the onset temperature and peak temperature of these polymers show that the thermal stability of nitro-HTPB is more than NHTPB, whereas nitrocellulose is slightly more thermally stable than nitro-HTPB (see Table 2). Also, the calculated values of kinetic and thermodynamic parameters (given in Table 3) confirm this trend.

Conclusions

Thermal behaviors of the nitro-HTPB samples containing different amounts of nitro groups were investigated utilizing simultaneous TG–DSC at nitrogen as the inert atmosphere. Thermoanalytical data revealed that the onset and maximum peak temperatures increased due to the higher nitro content in HTPB. Furthermore, increasing the DSC heating rate leads to the lower thermal stability temperatures of the nitro-HTPB. The Arrhenius parameters for 17.3 % nitro-HTPB were calculated by two different methods, i.e., ASTM and FWO using non-isothermal thermoanalytical data. Based on the resulted data, the half-life of 17.3 % nitro-HTPB at the temperature of 50 °C was predicted about 10 years. Meantime, the critical temperature of thermal explosion was computed as 181 °C.

References

1. Stacer RG, Husband DM. Molecular structure of the ideal solid propellant binder. *Propellants Explos Pyrotech.* 1991;16:167–76.
2. Manjari R, Joseph V, Pandureng L, Sriram T. Structure-property relationship of HTPB-based propellants. I. Effect of hydroxyl value of HTPB resin. *J Appl Polym Sci.* 1993;48:271–8.
3. Shamsipur M, Pourmortazavi SM, Hajimirsadeghi SS, Atifteh SM. Effect of functional group on thermal stability of cellulose derivative energetic polymers. *Fuel.* 2012;95:394–9.
4. Rocco JA, Lima JE, Frutuoso A, Iha K, Ionashiro M, Matos J, et al. TG studies of a composite solid rocket propellant based on HTPB-binder. *J Therm Anal Calorim.* 2004;77:803–13.
5. Muthiah R, Krishnamurthy V, Gupta B. Rheology of HTPB propellant. I. Effect of solid loading, oxidizer particle size, and aluminum content. *J Appl Polym Sci.* 1992;44:2043–52.
6. Mahkam M, Nabati M, Latifpour A, Aboudi J. Synthesis and characterization of new nitrogen-rich polymers as candidates for energetic applications. *Des Monomers Polym.* 2014;17:453–7.
7. Agrawal JP. Some new high energy materials and their formulations for specialized applications. *Propellants Explos Pyrotech.* 2005;30:316–28.
8. Badgajar D, Talawar M, Asthana S, Mahulikar P. Advances in science and technology of modern energetic materials: an overview. *J Hazard Mater.* 2008;151:289–305.
9. Agrawal JP. Some new high energy materials and their formulations for specialized applications. *Propellants Explos Pyrotech.* 2005;30:316–28.
10. Eroglu MS, Hazer B, Güven O. Synthesis and characterization of hydroxyl terminated poly(butadiene)-g-poly(glycidyl azide) copolymer as a new energetic propellant binder. *Polym Bull.* 1996;36:695–701.
11. Agrawal JP. Recent trends in high-energy materials. *Prog Energy Combust Sci.* 1998;24:1–30.
12. Colclough ME, Desai H, Millar RW, Paul NC, Stewart MJ, Golding P. Energetic polymers as binders in composite propellants and explosives. *Polym Adv Technol.* 1994;5:554–60.
13. Millar RW, Colclough ME, Desai H, Golding P, Honey PJ, Paul NC, Sanderson AJ, Stewart MJ. Novel syntheses of energetic materials using dinitrogen pentoxide. In: Albright LF, Carr RVC, Schmitt RJ, editors. *Nitration recent laboratory and industrial development*, ACS Symposium Series, vol. 623. 1996. p. 104–121 [Chapter 11].
14. Millar R, Colclough M, Golding P, Honey P, Paul N, Sanderson A, et al. New synthesis routes for energetic materials using dinitrogen pentoxide [and discussion]. *Philos Trans R Soc Lond Ser A Phys Eng Sci.* 1992;339(1654):305–19.
15. Talawar M, Sivabalan R, Anniyappan M, Gore G, Asthana S, Gandhe B. Emerging trends in advanced high energy materials. *Combust Explos Shock.* 2007;43:62–72.
16. Gaur B, Lochab B, Choudhary V, Varma I. Azido polymers—energetic binders for solid rocket propellants. *J Macromol Sci Part C Polym Rev.* 2003;43:505–45.
17. Millar RW, Philbin SP. Clean nitrations: novel syntheses of nitramines and nitrate esters by nitrodesilylation reactions using dinitrogen pentoxide. *Tetrahedron.* 1997;53:4371–86.
18. Chien J, Kohara T, Lillya C, Sarubbi T, Su BH, Miller R. Phase transfer-catalyzed nitromercuration of diene polymers. *J Polym Sci Polym Chem Ed.* 1980;18(8):2723–9.
19. Lugadet F, Deffieux A, Fontanille M. Synthèse de polybutadiènes nitrés hydroxytelechéliques par nitromercuration-démércuration. Etude de la démércuration et caractérisation des polybutadiènes nitrés. *Eur Polym J.* 1990;26:1035–40.
20. Pourmortazavi SM, Hajimirsadeghi SS, Hosseini SG. Characterization of the aluminum/potassium chlorate mixtures by simultaneous TG–DTA. *J Therm Anal Calorim.* 2006;84:557–61.
21. Pourmortazavi SM, Fathollahi M, Hajimirsadeghi SS, Hosseini SG. Thermal behavior of aluminum powder, potassium perchlorate mixtures by DTA, TG. *Thermochim Acta.* 2006;443:129–31.
22. Fathollahi M, Pourmortazavi SM, Hosseini SG. The effect of the particle size of potassium chlorate in pyrotechnic compositions. *Combust Flame.* 2004;138:304–6.
23. Hosseini SG, Pourmortazavi SM, Hajimirsadeghi SS. Thermal decomposition of pyrotechnic mixtures containing sucrose with either potassium chlorate or potassium perchlorate. *Combust Flame.* 2005;141:322–6.

24. Singh G, Kapoor IPS, Mannan SM, Kaur J. Studies on energetic compounds, Part 8: thermolysis of salts of HNO₃ and HClO₄. *J Hazard Mater.* 2000;A79:1–18.
25. Zeman S. New aspects of initiation reactivities of energetic materials demonstrated on nitramines. *J Hazard Mater.* 2006;A132: 155–64.
26. Keshavarz MH. Simple method for prediction of activation energies of the thermal decomposition of nitramines. *J Hazard Mater.* 2009;162:1557–62.
27. Shekhar Pant C, Santosh MS, Banerjee S, Khanna PK. Single step synthesis of nitro-functionalized hydroxyl-terminated polybutadiene. *Propellants Explos Pyrotech.* 2013;38:748–53.
28. Turner AG, Davis LP. Decomposition pathways leading to HONO for nitroalkenes. *J Energ Mater.* 1984;2:191–204.
29. ASTM E 698-05. Standard test method for Arrhenius kinetic constants for thermally unstable materials.
30. Sunitha M, Reghunadhan Nair C, Krishnan K, Ninan K. Kinetics of Alder-ene reaction of Tris(2-allylphenoxy) triphenoxycyclotriphosphazene and bismaleimides: a DSC study. *Thermochim Acta.* 2001;374:159–69.
31. Pourmortazavi SM, Kohsari I, Teimouri MB, Hajimirsadeghi SS. Thermal behaviour kinetic study of the dihydroglyoxime and dichloroglyoxime. *Mater Lett.* 2007;61:4670–4.
32. Shamsipur M, Pourmortazavi SM, Hajimirsadeghi SS. Investigation on decomposition kinetics and thermal properties of copper fueled pyrotechnic compositions. *Combust Sci Technol.* 2011;183:575–87.
33. Ma H, Yan B, Li Z, Guan Y, Song J, Xu K, et al. Preparation, non-isothermal decomposition kinetics, heat capacity and adiabatic time-to-explosion of NTO·DNAZ. *J Hazard Mater.* 2009;169:1068–73.
34. Roduit B, Xia L, Folly P, Berger B, Mathieu J, Sarbach A, et al. The simulation of the thermal behavior of energetic materials based on DSC and HFC signals. *J Therm Anal Calorim.* 2008;93: 143–52.
35. Pourmortazavi SM, Hosseini S, Rahimi-Nasrabadi M, Hajimirsadeghi S, Momenian H. Effect of nitrate content on thermal decomposition of nitrocellulose. *J Hazard Mater.* 2009;162: 1141–4.
36. Pourmortazavi SM, Hajimirsadeghi SS, Kohsari I, Fathollahi M, Hosseini SG. Thermal decomposition of pyrotechnic mixtures containing either aluminum or magnesium powder as fuel. *Fuel.* 2008;87:244–51.
37. Pisharath S, Ang HG. Synthesis and thermal decomposition of GAP–Poly (BAMO) copolymer. *Polym Degrad Stab.* 2007;92(7): 1365–77.
38. Rocco J, Lima J, Frutuoso A, Iha K, Ionashiro M, Matos J, et al. Thermal degradation of a composite solid propellant examined by DSC. *J Therm Anal Calorim.* 2004;75:551–7.
39. Salla J, Morancho J, Cadenato A, Ramis X. Non-isothermal degradation of a thermoset powder coating in inert and oxidant atmospheres. *J Therm Anal Calorim.* 2003;72(2):719–28.
40. Olszak-Humienik M, Mozejko J. Thermodynamic functions of activated complexes created in thermal decomposition processes of sulphates. *Thermochim Acta.* 2000;344:73–9.
41. Tompa AS, Boswell RF. Thermal stability of a plastic bonded explosive. *Thermochim Acta.* 2000;357:169–75.
42. Shamsipur M, Pourmortazavi SM, Roushani M, Miran Beigi AA. Thermal behavior and non-isothermal kinetic studies on titanium hydride-fueled binary pyrotechnic compositions. *Combust Sci Technol.* 2013;185:122–33.
43. Pickard JM. Critical ignition temperature. *Thermochim Acta.* 2002;392:37–40.
44. Tonglai Z, Rongzu H, Yi X, Fuping L. The estimation of critical temperatures of thermal explosion for energetic materials using non-isothermal DSC. *Thermochim Acta.* 1994;244:171–6.
45. Tonglai Z, Rongzu H, Yi X, Fuping L. The estimation of critical temperatures of thermal explosion for energetic materials using non-isothermal DSC. *Thermochim Acta.* 1994;244:171–6.
46. Shamsipur M, Pourmortazavi SM, Fathollahi M. Kinetic parameters of binary iron/oxidant pyrolants. *J Energ Mater.* 2012;30: 97–106.
47. Wang Q, Wang L, Zhang X, Mi Z. Thermal stability and kinetic of decomposition of nitrated HTPB. *J Hazard Mater.* 2009;172(2): 1659–64.